

## INVESTIGATION OF FERROUS CONGLOMERATE PARTICLES FOUND IN CARWASH SLURRY AND THEIR ENVIRONMENTAL IMPLICATIONS

**Simona Elena AVRAM<sup>a</sup>, Miuta Rafila FILIP<sup>b,\*</sup>,  
Lucian BARBU TUDORAN<sup>c,d</sup>, Gheorghe BORODI<sup>d</sup>,  
Ioan PETEAN<sup>e,\*</sup>**

**ABSTRACT.** Ferrous particles are usually found in atmospheric particulate matters due to the cars chassis oxidation. These particles are able forming conglomerates with the other mineral particles. Thus, the investigated carwash slurry (CS) reveals a high mineralized composition dominated by Quartz, Calcite and clay minerals with significant amount of iron hydroxides. We found some unusual bigger particles of ferrous conglomerate (FC) into the CS sample. XRD and mineralogical microscopy (MOM) reveal that FC sample is formed by a nanostructured mixture of 56 wt.% Calcite and 44 wt.% Goethite. SEM images and EDS spectra reveal submicron particles within the FC structure with a dense mixture of Ca and Fe. FTIR investigation reveal strong absorption bands for goethite and very weak ones for Lepidocrocite within the FC sample. The results indicates that the conglomerate was formed on the car chassis rust by wet partial dissolution of calcite that locally forms  $\text{Ca}(\text{OH})_2$  which further is re-crystallized as calcite due to the  $\text{CO}_2$  from the combustion gases. Fine crystallites of iron hydroxides are embedded into the re-crystallized

---

<sup>a</sup> Faculty of Materials and Environmental Engineering, Technical University of Cluj-Napoca, 103-105 Muncii Bd., RO-400641, Cluj-Napoca, Romania.

<sup>b</sup> Raluca Ripan Institute for Research in Chemistry “, Babes-Bolyai University, 30 Fantanele Street, 400294 Cluj-Napoca, Romania.

<sup>c</sup> Faculty of Biology and Geology, Babes-Bolyai University, 44 Gheorghe Bilaşcu Street, 400015 Cluj-Napoca, Romania.

<sup>d</sup> National Institute for Research and Development of Isotopic and Molecular Technologies, 65-103 Donath Street, 400293 Cluj-Napoca, Romania.

<sup>e</sup> Faculty of Chemistry and Chemical Engineering, Babes-Bolyai University, 11 Arany Janos Street, 400028 Cluj-Napoca, Romania.

\* Correspondent authors: [miuta.filip@ubbcluj.ro](mailto:miuta.filip@ubbcluj.ro); [ioan.petean@ubbcluj.ro](mailto:ioan.petean@ubbcluj.ro)



calcite. In conclusion, the magnetic selection is recommended for the ferrous conglomerate particles removal from CS to be used as natural coverage for of urban dump sites rehabilitation.

**Keywords:** *Particulate Matters, ferrous conglomerate, environment*

## INTRODUCTION

Particulate matter (PM) represents a major environmental concern due to their ability to penetrate into the respiratory system and therefore to affect living beings' health [1, 2]. Particles size is one of the most important parameter regarding particulate matters. Particles with aerodynamic diameter of 10  $\mu\text{m}$  are standardized as PM10; those having 2.5  $\mu\text{m}$  are PM2.5 [3, 4]. New environmental trends try to bring on the standards PM1 class with an aerodynamic diameter of 1  $\mu\text{m}$  and below. Fact is really difficult because the lack on precise quantitative measuring of such finest particles amount [5, 6]. Some of the newest research in the field reveals nanostructural fractions within particulate matter samples [7 - 9].

Carwash slurry collects all kind of PM related to the streets traffic and reflects the particles movements during suspension – sedimentation – re suspension cycles [10, 11]. Thus, a lot of atmospheric suspended particles sediments on the cars surface containing significant amounts of PMs' from PM1 to PM10. These particles have various sources such as: soil erosion [12, 13] generating mostly mineral components and generally associated with street dust [10, 14]; some local anthropogenic industrial activities [15, 16] and finally one of the most important is the circulating vehicles wear implying chassis rust [17, 18] and tires intensive usage [19, 20]. Some research relates ferrous conglomerates presence into the street dust due to the mineral particle's interactions with iron hydroxides on the car chassis rust scale evidencing embedding mainly small micro sized quartz slivers and traces of clays [9, 21].

Present research is focused on some unusual bigger particles of ferrous conglomerate found in carwash slurry resulted from a large facility deserving all kind of road vehicles such as: cars, buses and heavy lorry which circulates on average and long cruises covering the Euro – Region 6 NV in Romania. It implicates mainly sedimentary soils specific to the Transylvanian Basin based on minerals like: Quartz, Calcite, and clays (e.g. Muscovite and Kaolinite) [22, 23]. Large areas within the coverage area are dominated by evaporitic formations such as sodium chloride crystallized as Halite [24 – 25].

We aim to investigate the physicochemical composition and microstructure of these ferrous conglomerate particles and their relation with the carwash slurry and their further environmental implications.

## RESULTS AND DISCUSSION

The mineral composition of the samples was investigated by X – ray diffraction (XRD) correlated with mineralogical optical microscopy (MOM) assuring a complete view of the mineral distribution within the samples. The XRD pattern resulted for carwash slurry sample (CS) is presented in Figure 1a. It has a profound crystalline nature dominated by very well-developed peaks with significant intensities and narrow allure. There are also observed some small broadened peaks which may belong to small particles or to some nano-crystalline formations. The dominant mineral is Quartz followed closely by Calcite, Kaolinite and Muscovite. We notice that cumulative clay amount is situated just after Quartz overtaking Calcite position. Some of the clay diffraction peaks are intense and narrow indicating presence of large particles but also some of them are slightly broadened indicating the presence of fine submicron clay particles as well. There were identified relevant peaks for Goethite (e.g.  $\alpha$  Iron Hydroxide) and some traces of Lepidocrocite (e.g.  $\gamma$  Iron Hydroxide). Each mineral amount in CS sample was established by Reference Intensity Ratio RIR method measuring relative intensities and minerals corundum factor [26, 27]. The obtained values are centralized in Table 1.

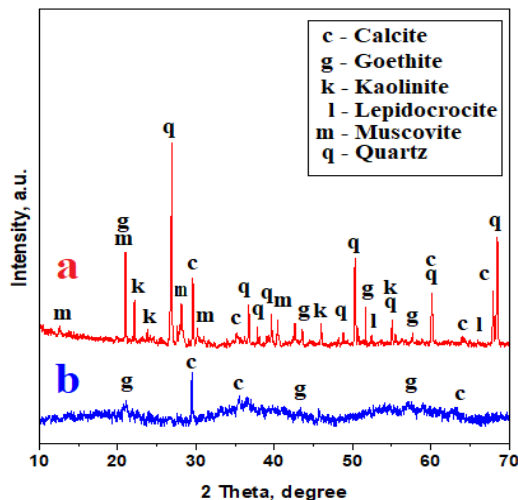


**Figure 1.** The XRD patterns for: a) carwash slurry and b) ferrous conglomerate.

The ferrous conglomerate sample (FC) presents a XRD pattern with less intense peaks and very broadened due to the presence of nano-crystalline structure, Figure 1b. The dominant mineral is Calcite followed by Goethite indicating a very strange composition. The usual iron conglomerates found in urban street dust related to the cars chassis corrosion are dominated by iron hydroxides mixture (e.g. Goethite and Lepidocrocite) which embeds mainly quartz fine fresh broken particles and clays traces up to 30 wt. % [9, 21]. Now, FC sample has 56 wt.% Calcite and 44 wt.% Goethite according to RIR determination, Table 1. It means that Calcite embeds the Goethite crystals. Therefore, we calculate the crystallite size using Scherrer Formula [7, 10] resulting a mean diameter of 40 nm for Calcite and 60 nm for Goethite. The fact is very strange since the usual ferrous conglomerates related to the street dust are micro-aggregates instead of nanostructured composition.

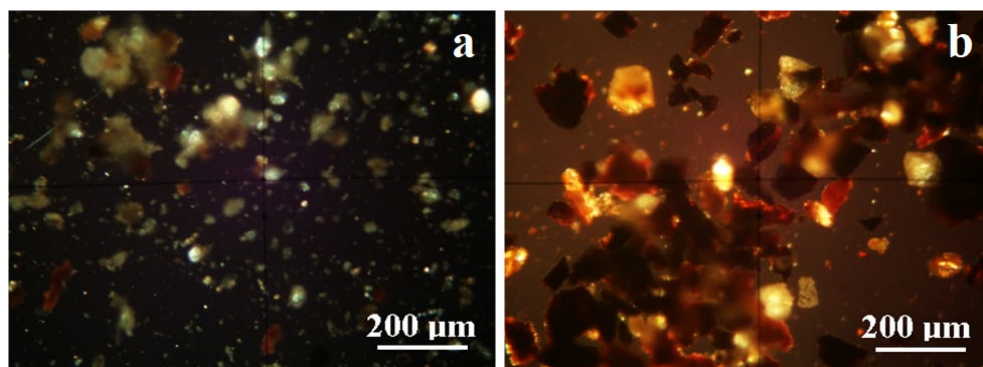


**Figure 2.** Mineralogical optical microscopy for: a) carwash slurry and b) ferrous conglomerate.

Mineral particles distribution within CS sample is observed in the MOM image in Figure 2a. Each mineral has its own color nuance allowing proper identification and particle size measurement, the obtained data being centralized in Table 1.

INVESTIGATION OF FERROUS CONGLOMERATE PARTICLES FOUND  
IN CARWASH SLURRY AND THEIR ENVIRONMENTAL IMPLICATIONS

**Table 1.** Samples mineral characteristics

Component	Quartz	Kaolinite	Muscovite	Calcite	Goethite	Lepidocrocite
Formula	SiO <sub>2</sub>	Al <sub>2</sub> Si <sub>2</sub> O <sub>5</sub> (OH) <sub>4</sub>	Al <sub>2</sub> K <sub>2</sub> O <sub>6</sub> Si	CaCO <sub>3</sub>	αFeO(OH)	γFeO(OH)
Carwash slurry						
Amount, wt. %	29	19	17	25	7	3
Particle size range, μm	5 - 50	5 - 65	1 - 30	1 - 25	5 - 30	5 - 30
Conglomerate						
Amount, wt. %	-	-	-	56	44	-
Particle size range, μm	-	-	-	3 - 100	5 - 100	-
Crystallite size, nm	-	-	-	40	60	-
Color in cross polarized light	Green - gray	White-blue	Pink	Yellow-brown	Reddish - brown	Reddish - brown
Particle shape	round	tabular	tabular	round	elongated	elongated

It results that all identified minerals have bigger particles which are classified as suspended particles (diameters from 10 up to 65 μm). They are accompanied by PM10 fractions which contain mainly Quartz and Calcite as well as few ferrous conglomerate particles (mixture of Goethite and Lepidocrocite traces). The PM2.5 fraction contains mainly clay particles such as Kaolinite and Lepidocrocite. The mineral composition and particle distribution of CS sample reveals that PM originates in the soil erosion in good agreement with literature [12, 13] excepting ferrous particles which rather originate in the cars rust in good agreement with [17, 18]. All observed particles within CS sample have dark spots which belong to the amorphous organic phase that requires FTIR investigation.

On the other side, FC sample, Figure 2b, reveals uneven broken fractions of ferrous conglomerate. The light-yellow particles belong to Calcite that embeds different amount of Goethite (reddish brown). In consequence, come of the particles present red color and the ones with densest embedding of iron hydroxide appear dark brown.

SEM image of CS sample, Figure 3a, reveal a particle distribution similar to the one observed by MOM. Bigger particles (Quartz and Calcite) are surrounded by fine clay particles, fact sustained by the elemental map.

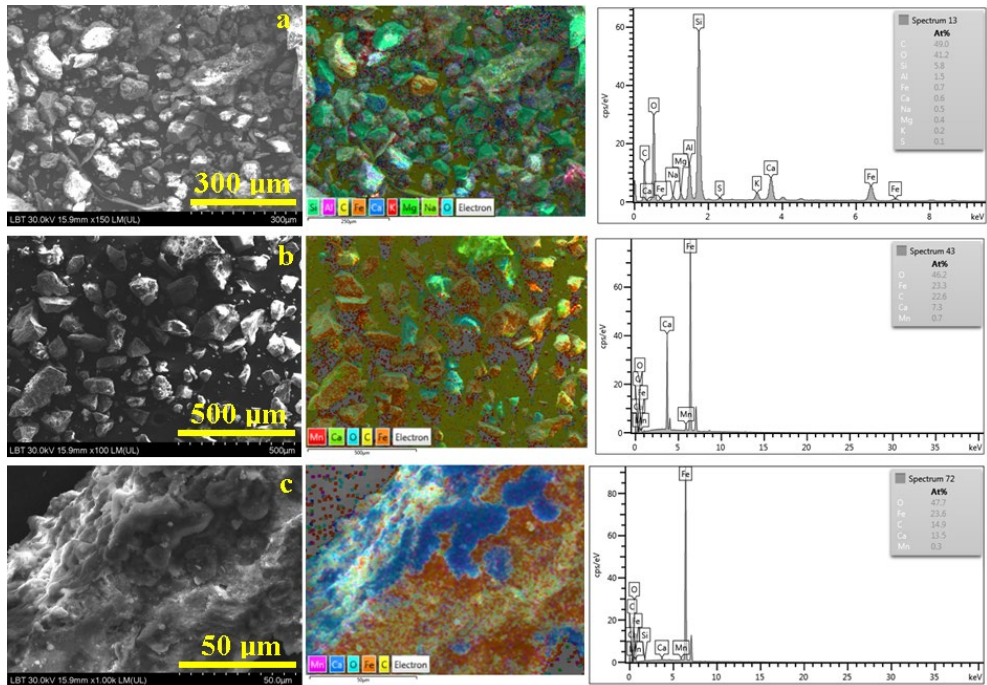


**Figure 3.** SEM images with elemental maps and EDS spectra for a) carwash slurry, b) ferrous conglomerate and c) details on a single ferrous conglomerate particle.

The elemental map sustains the mineral assignment to the observed particles: Quartz particles appear bright green due to the Si labeled green and O labeled cyan; Calcite particles appear in dark blue nuance because Ca is labeled in dark blue. Fine clay particles are colored in dark red due to the presence of Al, K with small traces of Mg and Na. Particles colored in orange nuance belongs to the ferrous conglomerate because of orange labeling of Fe. The complete elemental composition of the CS sample is given in Table 2. Several yellow stains are observed on the particle surface indicating high concentration of non mineralized carbon that might be related with organic dirt spots identified by MOM. The presence of organic matter is sustained by very high amount of carbon resulted on the elemental composition

of CS sample. Oxygen amount is also high in CS and it is divided between organic matter and mineral oxides and silicates evidenced. The amount of 0.7 at. % Fe is in good agreement with the presence of the rusty particle of about 50  $\mu\text{m}$  diameter in Figure 3a.

**Table 2.** Samples elemental composition

Samples	Elemental composition, At. %										
	C	O	Si	Al	Fe	Ca	Na	Mg	K	S	Mn
CS	49	41	5.8	1.5	0.7	0.6	0.5	0.4	0.2	0.1	-
FC	22.6	46.2	-	-	23.3	7.3	-	-	-	-	0.7
Single FC particle	14.9	47.7	-	-	23.6	13.5	-	-	-	-	0.3

Figure 3b reveals the SEM aspect of broken particles within FC sample that are in good convergence with MOM observations in Figure 2b. The elemental map labels indicate: orange – Fe; cyan – O; light green Ca and red – Mn. The color combination reveals the yellow-greenish particles of calcite with different embedded amount of Goethite represented by orange spots. Manganese presence as low trace into the elemental composition of FC sample might be related with the lower side of the car corrosion. The overall elemental composition of FC sample is given in Table 2. It is dominated by oxygen carbon and iron, fact in good agreement with the XRD and MOM results. However, it is necessary a closer look at a single FC particle detail for a more precise determination.

High magnification detail of a single FC particle is presented in Figure 3c. Ferrous conglomerate particle evidence growth layers on the left side of the observation field. Corresponding elemental map shows that these layers have blue nuance for Calcite and orange nuance for the embedded Goethite. Oblique position of the FP particle side allows us establish an average thickness of the growth layer of 6.8  $\mu\text{m}$ . The outer most layer aspect is better observed on the central and left side of the observation field in Figure 3c. There are observed rounded clusters of Goethite about 5 – 10  $\mu\text{m}$  in diameter embedded into the nanostructured Calcite mass. Fact is sustained by the small brown-orange dots observed in the elemental map on these specific areas. The elemental composition of the single FC particle reveals large amount of O and Fe corresponding to the Goethite clusters embedded into the calcite. The amount of C and Ca respects the Calcite stoichiometric proportion, fact in very good agreement with XRD observations. Also, low traces of manganese occur, perhaps due to the corrosion of some alloyed steel part.

FC particles growth layer by layer indicates a long-term process that involves Calcite and Goethite. Missing Lepidocrocite is also a strange aspect related to the investigated ferrous conglomerate. A closer look to the chemical bonds within the samples is required. Therefore, FTIR analysis was effectuated for both samples CS and FC, Figure 4.

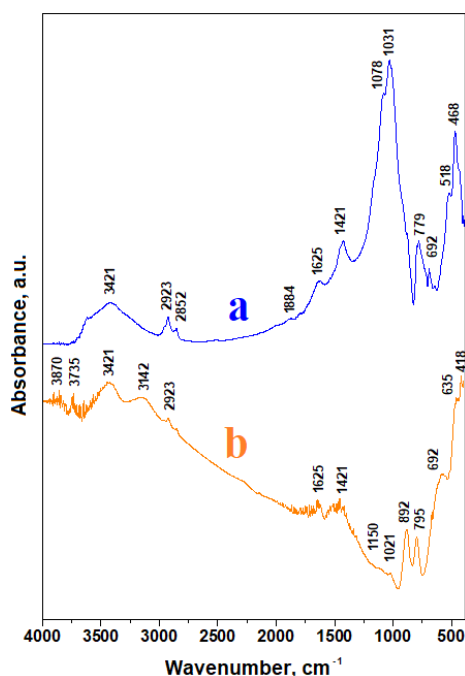


**Figure 4.** FTIR spectra for a) carwash slurry and b) ferrous conglomerate.

The first absorption bands resulted for CS sample, Figure 4a, belong to the mineral components: 468 cm<sup>-1</sup> is assigned to Si-O-Si deformation within silicates and clay, 518 cm<sup>-1</sup> corresponds to Fe-O chemical bond within iron oxides; 692 cm<sup>-1</sup> belongs to symmetrical deformation of CO<sub>3</sub><sup>2-</sup> within Calcite, 779 cm<sup>-1</sup> is assigned to Si-O stretching from Quartz, 1031 cm<sup>-1</sup> indicates the planar stretching of Si-O within silicates, 1421 cm<sup>-1</sup> reveals the asymmetric stretch of CO<sub>3</sub><sup>2-</sup> within Calcite [28, 29]. Water presence is related both to adsorbed water and chemically bonded molecules having absorption bands at: 1625 cm<sup>-1</sup> for H-O-H rotation and 3421 cm<sup>-1</sup> for H-O-H stretching [30].

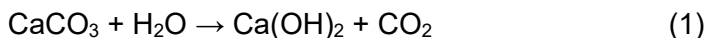
The other group of absorption bands within CS sample is related to the organic matter observed as dark amorphous spots in MOM images and rich carbon dots in SEM elemental maps. We found following bands at: 1078 cm<sup>-1</sup>

belonging to C-H deformation within CH<sub>3</sub> groups [31]; 1884 cm<sup>-1</sup> corresponding to symmetric stretch of the saturate C=O bond; 2852 cm<sup>-1</sup> assigned to symmetric stretch of CH<sub>2</sub> and 2923 cm<sup>-1</sup> belonging to asymmetric stretch of CH<sub>2</sub> [32, 33]. On the other side these absorption bands are related to the organic nanoparticles resulted from used tires [34, 35] and confirms the initial supposition that amorphous organic matter found in CS samples is mainly formed by tires nanostructural residues. Fact requires further detailed investigation with GC-MS techniques.

FTIR spectrum resulted for FC sample, Figure 4b, has a totally different allure that CS and evidenced different absorption bands. Some intense absorption bands are observed at 635; 795 and 892 cm<sup>-1</sup> characteristic for Goethite [36] followed by very weak absorption bands at 1021 and 1150 cm<sup>-1</sup> are reported for Lepidocrocite [36]. This particularly disposal of the absorption bands confirms the XRD observation that the Calcite prefer embedding of Goethite during the ferrous conglomerate growth due to its more stable structure [37, 38]. Calcite presence is evidenced by the following absorption bands: 692 cm<sup>-1</sup> related to the symmetric deformation of CO<sub>3</sub><sup>2-</sup> and 1421 cm<sup>-1</sup> related to asymmetric stretch of CO<sub>3</sub><sup>2-</sup> [29].

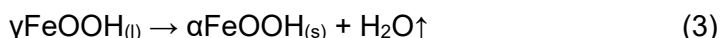
Water is also present in FC sample through the absorption bands at 1625 cm<sup>-1</sup> for H-O-H rotation and 3421 cm<sup>-1</sup> for H-O-H stretching [30] and some organic traces represented by the absorption bands: 2923 cm<sup>-1</sup> belonging to asymmetric stretch of CH<sub>2</sub> and OH stretching at 3735 cm<sup>-1</sup> [34, 35]. The presence of significant organic matter traces (induced by the cars used tires) in FC sample suggests that the conglomerate was formed by the street dust back scattered by the used tires in wet conditions that collides the rust scale.

Calcite might be partially dissolute under wet milling conditions induced by the tires and its aqueous solubility might be enhanced by the increased temperatures on the lower side of the cars chassis while Quartz particles are completely insoluble in water and tends to fell away due to impact forces. Furthermore, Calcite has a water solubility of 47 mg/L in the normal environmental condition. It might induce a partial dissolution of street dust calcite particles generating small amount of calcium hydroxide according to the reaction (1)

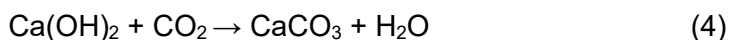


The calcium hydroxide embeds fine particles from rust scale containing iron hydroxides which are mainly Goethite and some traces of Lepidocrocite. The oxygen and hydroxyl anions are assembled in hexagonal crystallographic planes within Goethite assuring a better stability while in Lepidocrocite are arranged in cubic patterns within its orthorhombic lattice making

it less stable. Schwertmann and Taylor in 1972 described the transformation of Lepidocrocite into the Goethite in two steps: first is aqueous dissolution of Lepidocrocite followed by the re-crystallization of iron hydroxide into its more stable form as Goethite [38]. Lepidocrocite dissolution is described by relation (2),



while the Goethite crystallization from solution is described by relation (3). These processes are developed in rich  $\text{CO}_2$  atmosphere that facilitates reversing calcium hydroxide into calcite via equation (4):



re-crystallization process often found in the caves formations during sedimentary geological formations [39, 40]. When transformation from relations (3) and (4) occurs simultaneously the crystallized Goethite is embedded into the Calcite matrix forming a dense nanostructural pseudo-composite as observed in Figure 3c.

The obtained results are convergent and sustain the unusual composition and microstructure of the identified ferrous conglomerate figuring out some important environmental aspects. Physicochemical conditions required for the conglomerate formation needs large Calcite amounts which is provided by sedimentary soils erosion associated with advanced deforestations of high angle slope hills situated under research coverage area of Romanian Euro Region 6 NV. Auto-vehicles advanced rust of chassis bottom provide enough iron hydroxides for a consistent scale development that progressively interacts with calcite deposits facilitating multi-layered conglomerate development under high temperature that involved at average and long cruise. Tires also facilitate conglomerate deposits by the particularly grooves shape that spread the PM particles over the rusted chassis parts. Advanced wear of the tires also facilitates the emission of pollutant organic nanoparticles [41, 42] that affects both ferrous conglomerate and carwash slurry.

The environmental management regarding such carwash slurries implies two actions ways: the first is related to their proper dumping with care to avoid pollutant emissions and the second way is related to the particulate sources' mitigation strategies. Thus, the slurry dumping requires specialized dumps with consolidated deposited layers to avoid their sliding and with a strict humidity control of the top layers to avoid dust formation.

Hence, most of the minerals identified into the CS sample originate in the eroded soils the slurry might be converted to a stabile soil useful for urban dumps coverage during the conservation process. Some preliminary preparation actions are required: the ferrous conglomerate particles might negatively affect the further soil stability and could be separated by magnetic methods. Such methods were tested in laboratory for ferrous conglomerate removal from urban anti –skid material [43]. The carwash slurry sample free of ferrous rusted particles might be enhanced with humic components to link the finest clay particles into a stabilization network which might be effective at low humidity grades. Such pseudo-soil mixture might sustain some bushes vegetation like Sea Buckthorn (*Hippophae rhamnoides*) and Wild Rose (*Rosa Canina*) or even some trees like Pine (*Pinus Silvestris*) that were successfully used for coal sterile dumps stabilization [44, 45].

The carwash slurry PM mineral sources mitigation would imply major environmental actions such as eroded soils rehabilitation by re-forestation with young trees. Ferrous conglomerate mitigation could be achieved by removing from circulation old and rusted vehicles and by development of a proper anti – corrosive protection for the circulating vehicles to be applied on the lower side of the chassis. The organic particles emissions related to the tires might be mitigated by a proper choosing of the high thermal stability tires perfectly adapted to the geological conditions of the cruise area.

## CONCLUSIONS

Carwash slurry has a complex mineralogical composition resulted mostly due to the soil erosion. It is dominated by Quartz followed closely by Calcite and clay minerals (Kaolinite and Muscovite). There are also occur significant amounts of iron hydroxides: mainly Goethite and low traces of Lepidocrocite. The unusual ferrous conglomerate is formed by 56 wt.% Calcite in a nanostructured form having crystallites of about 40 nm that embeds an amount of 44 wt. % Goethite as nano-crystallites with mean diameter of 60 nm.

Carwash slurry might be reutilized as raw material for urban dumps rehabilitation if the ferrous conglomerate particles would be removed via magnetic selection. Also, its amount might be mitigated by proper environmental management including: eroded soil rehabilitation by re-forestation, anticorrosive protection of the lower side of vehicles chassis combined with withdrawing from circulation of old and depreciated cars. Organic matter related to the tire wear emission might be mitigated by a proper choosing of high thermal stability tires adapted on the geological conditions of the cruising areas.

## EXPERIMENTAL SECTION

A large carwash slurry sample (CS) was collected from a large washing facility for: cars, buses and heavy lorry deserving a wide coverage area within Romanian Euro Region 6 NV. The facility name and operator is anonymized for economical reasons.

The ferrous conglomerate (FC) sample was separated by sewing form the CS using a 4 mm mesh sieve and mechanical vibration device, followed by a manual selection according to their general brown – rusty aspect. The FC particles were further grinded manually into an agate mortar to obtain the powder necessary for specific analysis.

The X – ray diffraction analysis was effectuated with a Bruker D8 Advance diffractometer (Bruker Company, Germany) using  $\text{CuK}_{\alpha 1}$  radiation ( $\lambda = 1.54056 \text{ \AA}$ ) coupled with a monochromatic filter of Fe 40  $\mu\text{m}$ . The XRD patterns were registered in 2 Theta ranges of 10 – 70 degrees with a speed of 1 degree/minute. The minerals were identified using Match 1.0 software equipped with PDF 3.0 Powder Diffraction Files (Crystal Impact Company, Bonn, Germany).

Mineralogical Optical Microscopy (MOM) was effectuated with a Laboval 2 microscope (Carl Zeiss Jena, Oberocken, Germany) equipped with digital capture Kodak 10 Mpx camera. Quantitative analysis on the optical microphotographs was done using the Image J professional soft as freeware resource from National Institutes of Health USA.

Scanning Electron Microscopy was effectuated with a Hitachi SU8230 SEM (Tokyo, Japan), equipped with an EDX elemental analysis module X-Max 1160 EDS Energy-Dispersive Spectroscopy (Oxford Instruments, U.K.). The investigation was effectuated in high vacuum mode at an electron beam acceleration voltage of 30 kV.

Fourier Transformed Infrared spectroscopy FTIR was effectuated using a JASCO 610 FTIR (Jasco Corporation, Tokyo, Japan) under ambient conditions using the KBr pellet method in the range of 4000 – 400  $\text{cm}^{-1}$  at a resolution of 4  $\text{cm}^{-1}$  and 100 scans for each spectrum.

## REFERENCES

1. S.H. Pradhan, M. Gibb, A.T. Kramer, C.M. Sayes, *Environ. Res.*, **2023**, 231, 116267.
2. J. Qin, J. Wang, *Environ. Res.*, **2023**, 233, 116162.
3. V. Iyer, P.C. Ghosh, S. Ganapathy, K.C. Premarajan, *Saf. Health Work*, **2022**, 13, S204.
4. M. T. Udristoiu, Y. EL Mghouchi, H. Yildizhan, *J Clean. Prod.*, **2023**, 421, 138496.

INVESTIGATION OF FERROUS CONGLOMERATE PARTICLES FOUND  
IN CARWASH SLURRY AND THEIR ENVIRONMENTAL IMPLICATIONS

5. S. Wu, J. Tao, N. Ma, Y. Kuang, Y. Zhang, Y. He, Y. Sun, W. Xu, J. Hong, L. Xie, Q. Wang, H. Su, Y. Cheng, *Atmos. Environ.*, **2022**, 277, 119086.
6. H. Cigánková, P. Mikuška, J. Hegrová, J. Krajčovič, *Sci. Total Environ.*, **2021**, 800, 149502.
7. G. A. Păltinean, I. Petean, G. Arghir, D. F. Muntean, L.-D. Boboș, M. Tomoiaia-Cotișel, *Part. Sci. Technol.*, **2016**, 34, 580-585.
8. G. A. Păltinean, I. Petean, G. Arghir, D. F. Muntean, M. Tomoiaia-Cotișel, *Rev. Chim.*, **2016**, 67 (6), 1118-1123.
9. D. F. Muntean, D. Ristoiu, G. Arghir, R. F. Campean, I. Petean, *Carpathian J. Earth Environ. Sci.*, **2012**, 7, 175-182.
10. M. Rusca, T. Rusu, S. E. Avram, D. Prodan, G.A. Paltinean, M. R. Filip, I. Ciotlaus, P. Pascuta, T.A. Rusu, I. Petean, *Atmosphere*, **2023**, 14, 862.
11. V. M. Kolesnikova, O. A. Salimgareeva, D. V. Ladonin, V. Y. Vertyankina, A.S. Shelegina, *Atmosphere*, **2023**, 14, 403.
12. M. Tian, J. Gao, L. Zhang, H. Zhang, C. Feng, X. Jia, *Atmos. Pollut. Res.*, **2021**, 12, 101108.
13. A. A. Keri, T. Rusu, S. Avram, *Studia UBB. Ambientum*, **2010**, 55, 43-53.
14. A. Ghosh, P. K. Nagar, B. Singh, M. Sharma, D. Singh, *Sci. Total Environ.*, **2023**, 904, 167363.
15. S. Nicoara, L. Tonidandel, P. Traldi, S. Avram, O. Popa, N. Palibroda, *Studia UBB. Ambientum*, **2008**, 2, 186-192.
16. A. A. Keri, S. Avram, T. Rusu, *ProEnvironment*, **2010**, 3, 318-321.
17. M. Kadowaki, H. Katayama, *Corrosion Science*, **2023**, 222, 111379.
18. M. S. Sulaiman, D.A. Wahab, Z. Harun, H. Hishamuddin, N. K. Khamis, M. R. Abu Mansor, *Energy Rep.*, **2023**, 9, 235-246.
19. R. S. Cheong, E. Roubeau Dumont, P. E. Thomson, D. C. Castañeda-Cortés, L. M. Hernandez, X. Gao, J. Zheng, A. Baesu, J. R. Macairan, A. J. Smith, H. N. N. Bui, H.C.E. Larsson, S. Ghoshal, S. Bayen, V. S. Langlois, S.A. Robinson, N. Tufenkji, *J. Hazard. Mat. Adv.*, **2023**, 12, 100357.
20. I. Gehrke, S. Schläfle, R. Bertling, M. Öz, K. Gregory, *Sci. Total Environ.*, **2023**, 904, 166537.
21. D.F. Muntean, I. Ivan, L. Muresan, *Studia UBB Chemia*, **2015**, 60, 207-218.
22. C. Krézsek, A.W. Bally, *Mar. Pet. Geol.*, **2006**, 23, 405-442.
23. R. S. Huismans, G. Bertotti, D. Ciulavu, C. A. E. Sanders, S. Cloetingh, C. Dinu, *Tectonophysics*, **1997**, 272, 249-268.
24. L. Rus, S. E. Avram, V. Micle, *Studia UBB Chemia*, **2020**, 65, 257-268.
25. S. E. Avram, L. Rus, V. Micle, S. S. Hola, *Water*, **2022**, 14, 2366.
26. I. Petean, G. A. Paltinean, E. Pripon, G. Borodi, L. Barbu Tudoran, *Materials*, **2022**, 15, 7514.
27. I. Petean, G. A. Paltinean, A. C. Taut, S. E. Avram, E. Pripon, L. Barbu Tudoran, G. Borodi, *Materials*, **2023**, 16, 5809.
28. M. Lettieri, *Vib. Spectros.*, **2015**, 76, 48-54.
29. K. Koupadi, S.C. Boyatzis, M. Roumpou, N. Kalogeropoulos, D. Kotzamani, *Heritage*, **2021**, 4, 3611.
30. J. Bora, P. Deka, P. Bhuyan, K. P. Sarma, R. R. Hoque, *SN Appl. Sci.*, **2021**, 3, 137.

31. A. M. Udrea, A. Dinache, J. M. Pagès, R.A. Pirvulescu, *Molecules*, **2021**, 26, 2374.
32. X. Liu, S. M. Colman, E. T. Brown, E.C., Minor, H. Li, *J. Paleolimnol*, **2013**, 50, 387-398.
33. F. Usman, B. Zeb, K. Alam, Z. Huang, A. Shah, I. Ahmad, S. Ullah, *Atmosphere*, **2022**, 13, 124.
34. G. Sarkissian, J. Keegan, E. Du Pasquier, J. P. Depriester, P. Rousselot, *J. Can. Soc. Forensic Sci.*, **2004**, 37, 19-37.
35. Z. Wang, M. Wu, G. Chen, M. Zhang, T. Sun, K. G. Burra, S. Guo, Y. Chen, S. Yang, Z. Li, T. Lei, A. K. Gupta, *Fuel*, **2023**, 337, 127206.
36. H. Ciu, W. Ren, P. Lin, Y. Liu, *J. Experim. Nanosci.*, **2013**, 8, 869-875.
37. Y. Cudennec, A. Lecerf, *Solid State Sci.*, **2005**, 7, 520.
38. U. Schwertmann, R. M. Taylor, *Clays Clay Miner.*, **1972**, 20, 151-164.
39. O. T. Moldovan, S. Bercea, R. Năstase-Bucur, S. Constantin, M. Kenesz, I. C. Mirea, A. Petculescu, M. Robu, R. A. Arghir, *Tour. Manag.*, **2020**, 78, 104037.
40. C. Spötl, G. Koltai, Y. Dublyansky, *Chem. Geol.*, **2023**, 638, 121712.
41. S. H. Woo, H. Jang, S. H. Mun, Y. Lim, S. Lee, *Sci. Total Environ.*, **2022**, 838, 156548.
42. E. Roubeau Dumont, X. Gao, J. Zheng, J. Macairan, L. M. Hernandez, A. Baesu, S. Bayen, S. A. Robinson, S. Ghoshal, N. Tufenkji, *J. Hazard. Mat.*, **2023**, 453, 131402.
43. G. Arghir, I. Petean, D. F. Muntean, L. Muresan, C. Suci, *Powder Metall. Prog.*, **2011**, 11, 340-346.
44. A. Braşovan, V. Codrea, G. Arghir, R. F. Câmpean, I. Petean, *Carpathian J. Earth Environ. Sci.*, **2011**, 6, 221-228.
45. A. Braşovan, R. F. Burtescu, N. K. Olah, I. Petean, V. Codrea, A. Burtescu, *Studia UBB Chemia*, **2017**, 62(2), 81-93.